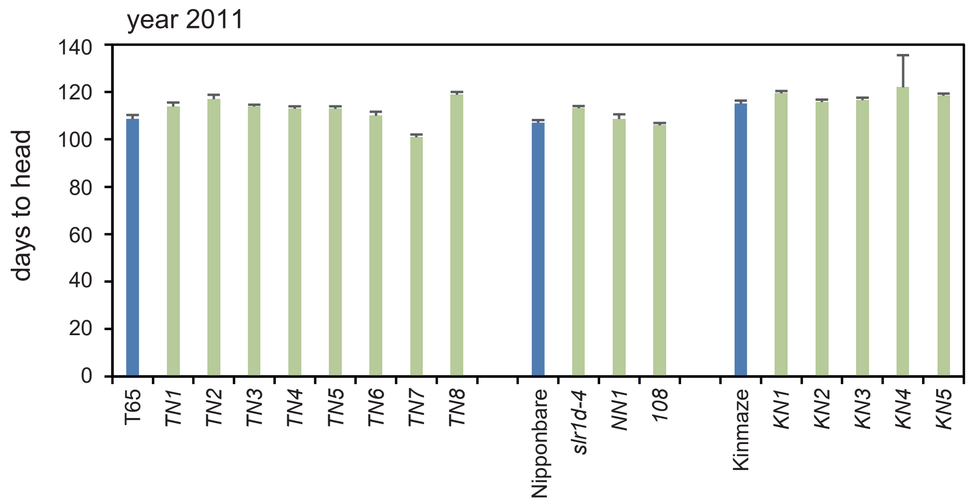

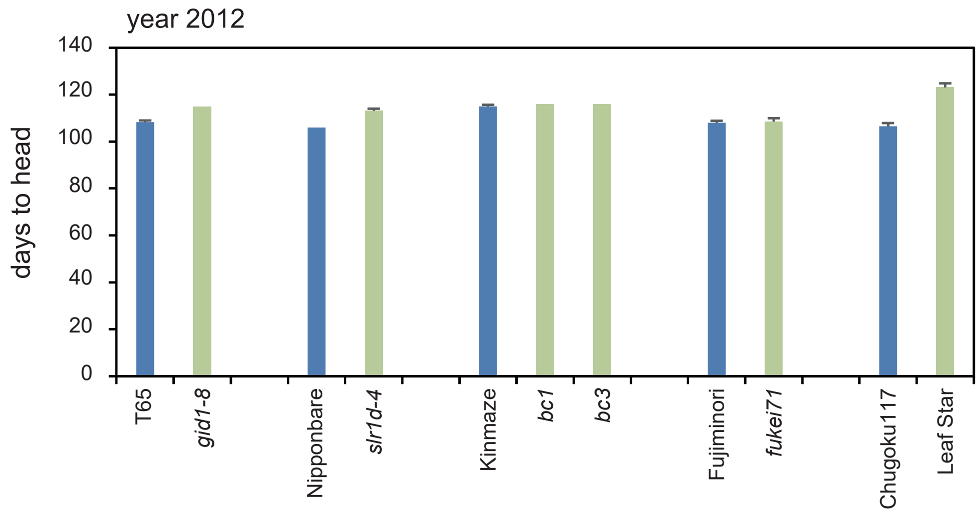

Fig. S1 Heading date of mutants used in this study in comparison to their original cultivars. Days to head of original cultivars and mutant lines are shown in blue and green bars, respectively. Three or more individual plants were used. Error bars indicate the standard error.

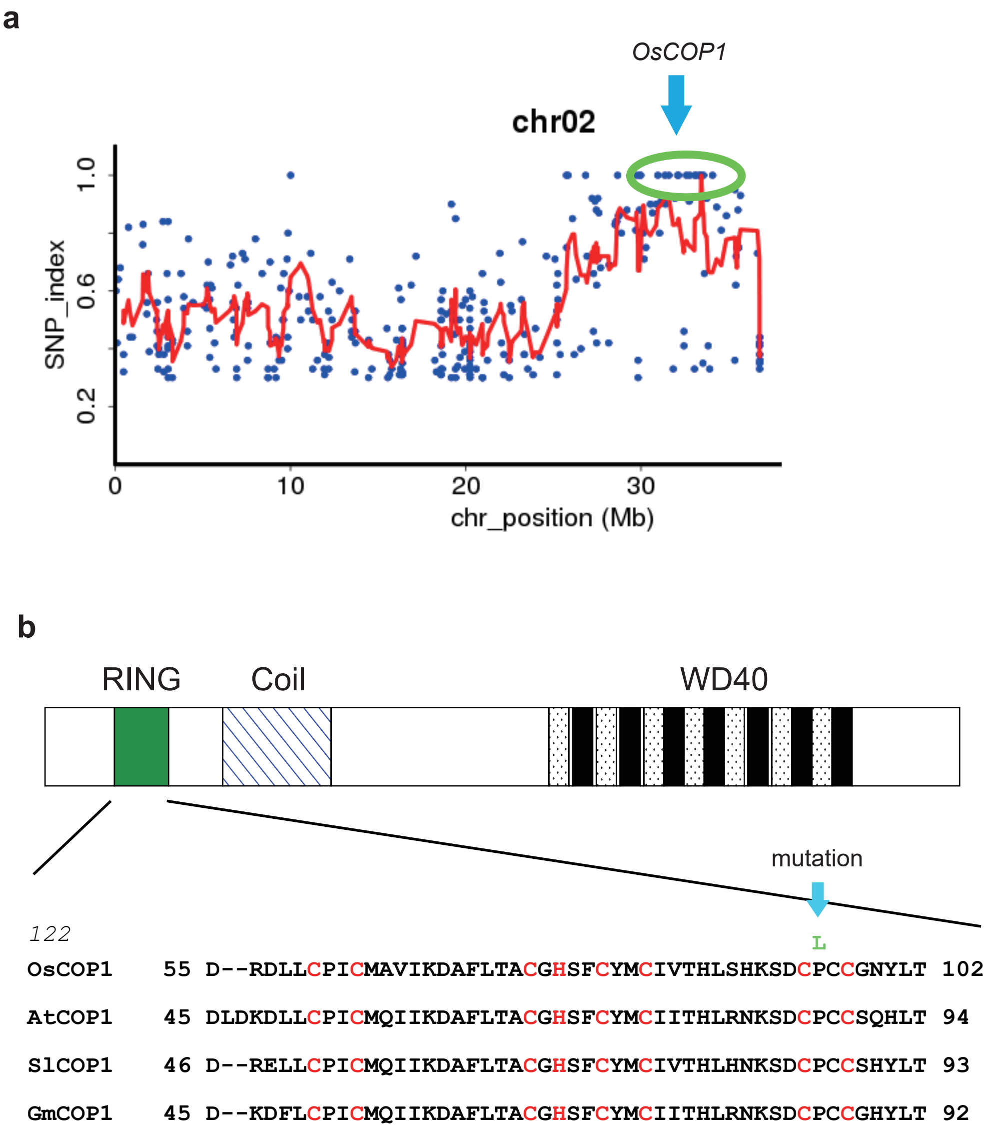

Fig. S2 MutMap analysis of *122*. **a** The SNP index of chromosome 2 as calculated from *122* and its parental cultivar T65 is represented by blue dots. Note that the SNP index = 1.0 is observed with high frequency at the 30 Mb region (green circle) and *OsCOP1* (green arrow) is located at 32.5 Mb. **b** Functional structure of OsCOP1 and the location of the *122* mutation. *122* contains a proline to leucine mutation in the RING-finger domain. Multiple sequence alignment of OsCOP1, AtCOP1, SlCOP1, and GmCOP1 refer to COP1 of rice, *Arabidopsis thaliana*, *Solanum lycopersicum*, and *Glycine max*, respectively. Note that the proline residue is conserved among angiosperms

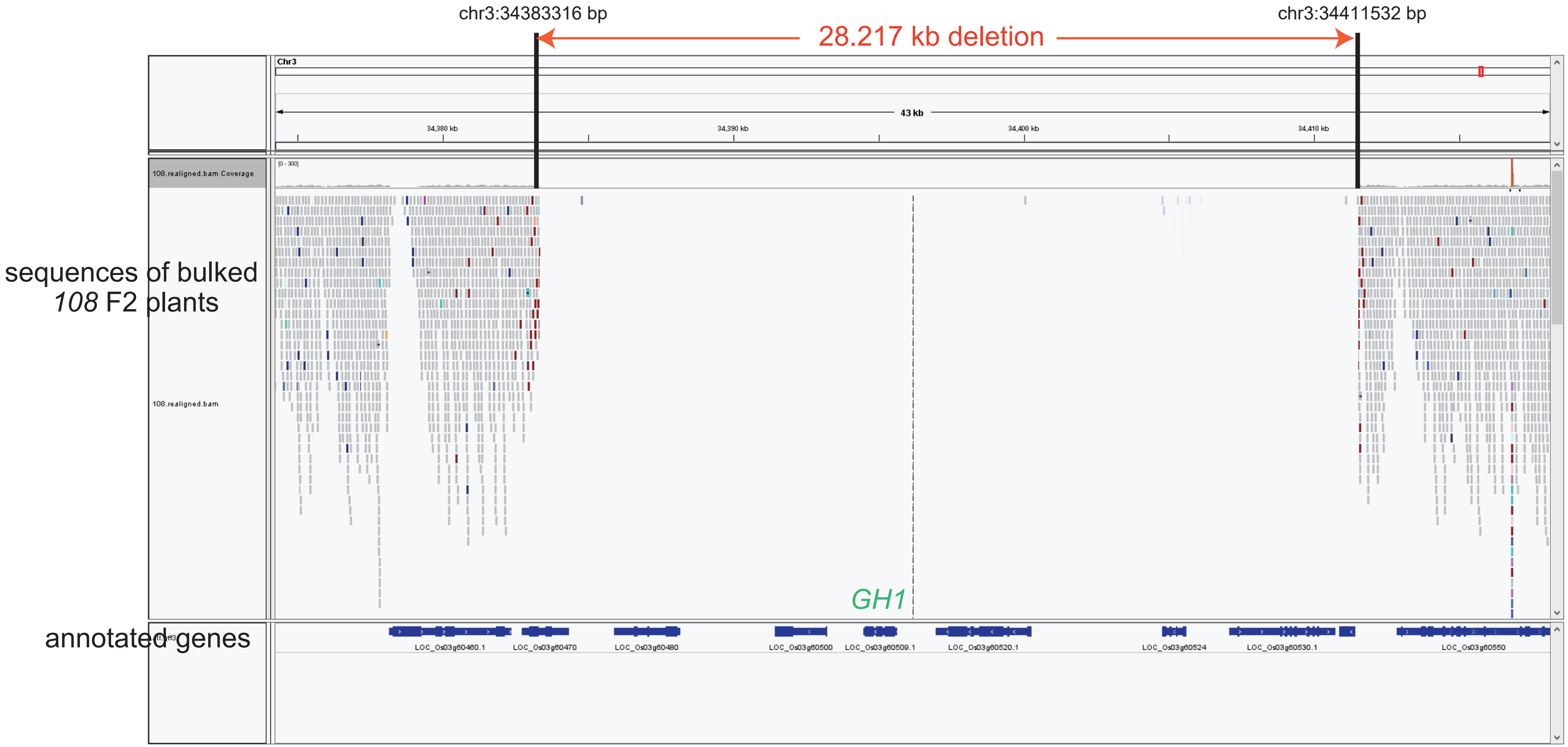

Fig. S3 Visualization of the read alignment of bulked *108* F2 DNA using Integrative Genomics Viewer (Thorvaldsdóttir et al. 2012). Sequences were aligned against the Nipponbare reference genome sequence, which was obtained from the TIGR database (ftp://ftp.plantbiology.msu.edu/pub/data/Eukaryotic_Projects/o_sativa/annotation_dbs/pseudomolecules/version_7.0/all.dir/). The region around the deletion (chromosome 3, location: 34383316-34411532) is presented. Note that individual sequences are aligned in the regions flanking the deletion (small rectangles). *GH1* maps within the deleted region

a

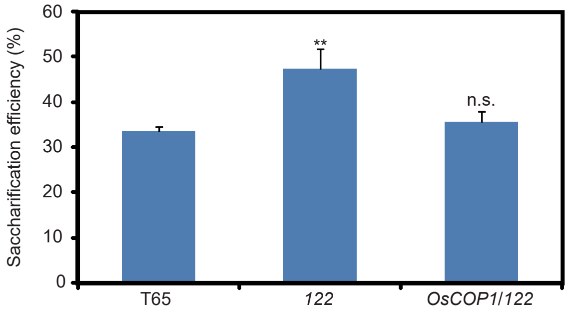

b

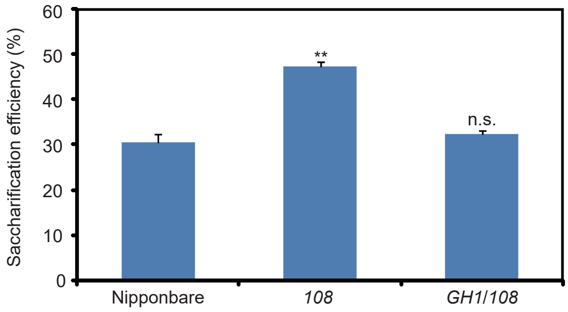

Fig. S4 Complementation of the *122* and *108* mutant phenotypes with *OsCOP1* and *GH1*, respectively. The introduction of *OsCOP1* and *GH1* restored the SE of *122* (**a**) and *108* (**b**) to the level exhibited by the original cultivars, respectively. n.s., not significantly different from original cultivar (**, $P < 0.01$; two-tailed Student's *t*-test)

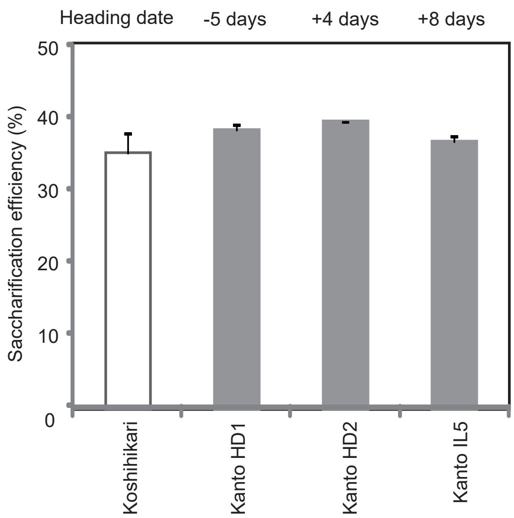

Fig. S5 Saccharification efficiency (SE) of Koshihikari and three near isogenic lines (NILs), Kanto HD1, Kanto HD2 and Kanto IL5. The days to heading of each NIL with respect to Koshihikari (0 day) is shown above the graph

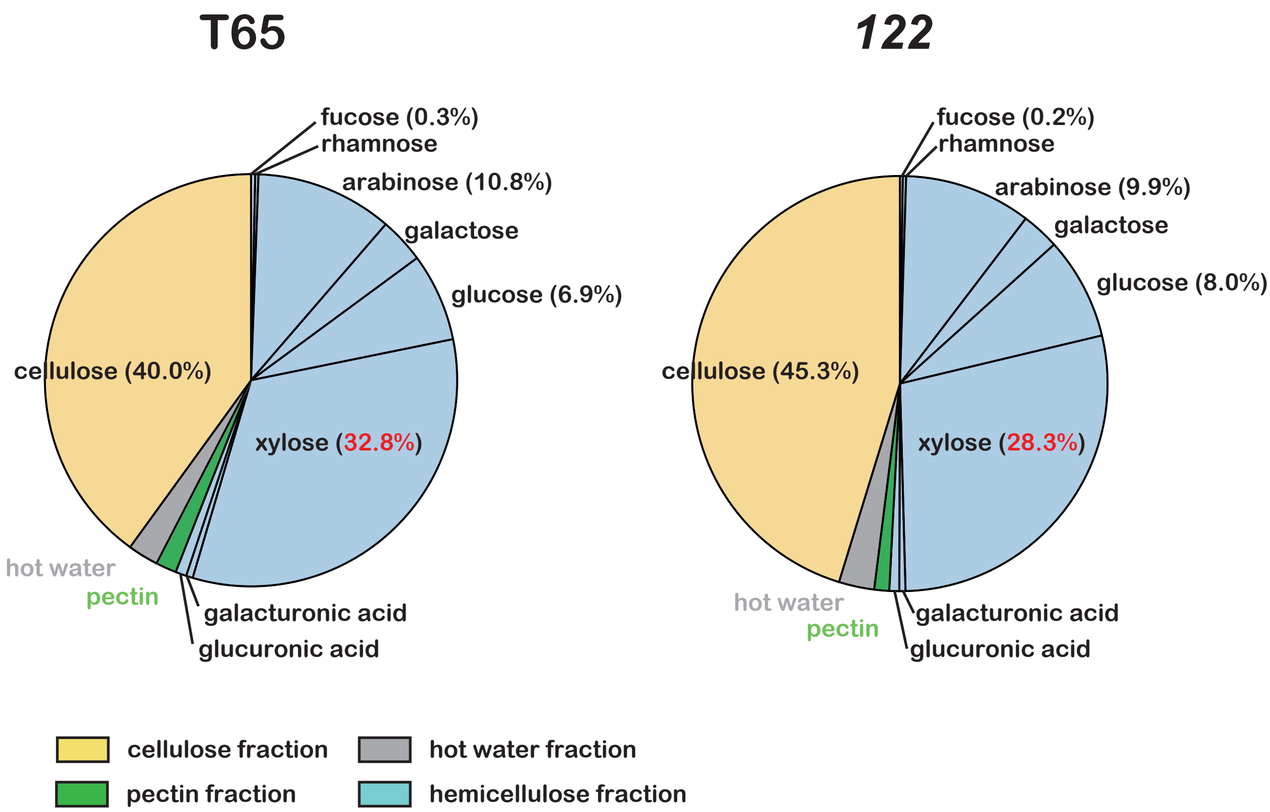

Fig. S6 Proportions of each cell wall fraction within the cell wall polysaccharides of *122* and its original cultivar T65. Sugar compositions of hemicellulose fraction (blue) against cell wall polysaccharides are also presented.

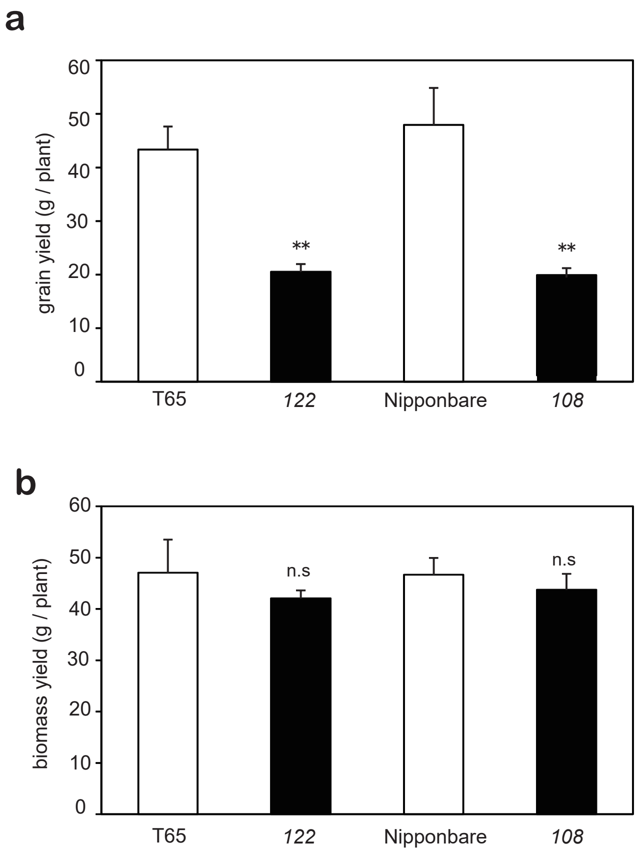

Fig. S7 Grain yield and biomass of *122*, *108* and their original cultivars (T65 and Nipponbare, respectively). Rice was sampled 40 days after heading, sun-dried for 2 weeks, and total grain yield (**a**) and biomass (excluding panicles and roots) (**b**) were measured (n=5). Asterisks indicate statistically significant differences with respect to the original cultivars (n.s., not significantly different from original cultivar. (**P < 0.01; two-tailed Student's t-test)

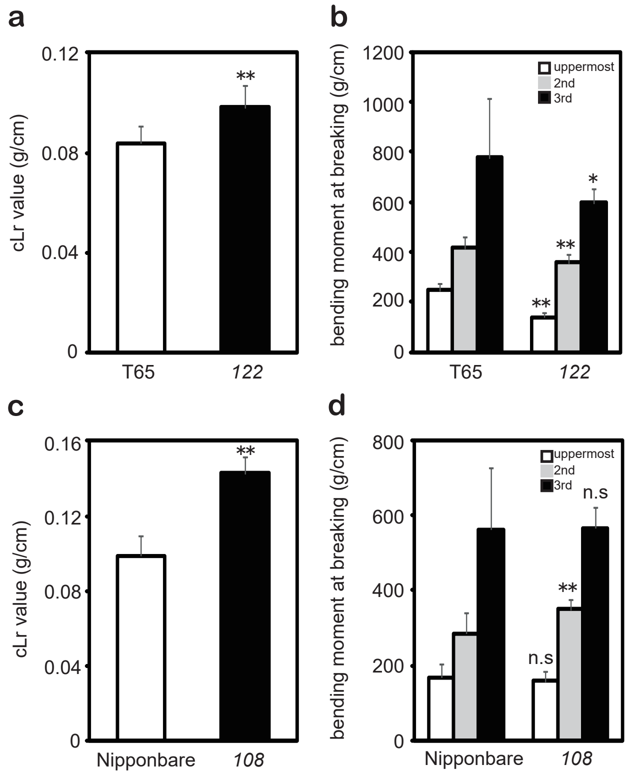

Fig. S8 Lodging resistance of *122* and *108* with their original cultivars (T65 and Nipponbare, respectively). Bending-type resistance was evaluated by the cLr value (**a**, **c**) and breaking-type resistance was evaluated by the BMB value (**b**, **d)**. 10 individuals were analyzed. Asterisks indicate statistically significant differences relative to the original lines (*$P < 0.05$, **$P < 0.01$; two-tailed Student's *t*-test)

Supplemental Table S1. Details of primers used for complementation analysis.

Primer	Sequence (5' to 3')	Note
AscI+OsCOP1 genome.F	GGCGCGCCAGGCAATTCAGTCAGCGTCT	5' primer amplifying *COP1* genome with *Asc* I site
OsCOP1 genome.R+AscI	GGCGCGCCTCAAAGAGAGCCGTGAACCT	3' primer amplifying *COP1* genomewith *AscI* site
SmaI+GH1.F	GGCCCGGGATGGCGGCCGTGTCGGAGG	5' primer amplifying *GH1* with *Sma* I site
GH1.R+SmaI	GGCCCGGGTCACGCGGACACCGGCGCG	3' primer amplifying *GH1* with *Sma* I site

Supplementary Table S2. Phenotypes of the mutants screened for improved SE.

brittle culm	original cultivar	other phenotypes	mutagen	references
bc1	Kinmaze	low cellulose, high lignin	unknown	Li et al. (2003)
bc3	Kinmaze	low cellulose	unknown	Hirano et al. (2010); Xiong et al. (2010)
122	T65	dark green leaf, thin uppermost internode	unknown	
flexible culm				
TN1	T65	curly and thin leaf, thin internode	unknown	
TN5	T65	mild golden culm and grain	unknown	
KN1	Kinmaze	pale greeen leaf	unknown	
KN5	Kinmaze	wide leaf	unknown	
TN7	T65	BR mutant like erect leaf	unknown	
TN8	T65		unknown	
brittle and flexible culm				
TN6	T65	shattering grain	unknown	
KN2	Kinmaze		unknown	
KN3	Kinmaze	drooping leaf	unknown	
KN4	Kinmaze	pale green leaf	unknown	
felxible culm and early senescence				
TN4	T65		unknown	
golden colored grain and internode				
108	Nipponbare	golden grain and internode	unknown	
early senescence				
TN3	T65	thin internode	unknown	
NN1	Nipponbare		unknown	
waxy leaf surface				
TN2	T65	short panicle	unknown	
ectopic accumulation of polysaccharide-linked FA and *p*CA				
fukei71	Fujiminori	low arabinose, low xylose, high glucose	unknown	Mase et al. (2005)
lignin deficient cultivar				
Leaf Star	Chugoku117	*cad2* mutant, low lignin	generated by breeding	Ookawa et al. (2014)
gibberellin mutant				
gid1-8	T65	GA receptor dwarf mutant	*N*-methyl-*N*-nitrosourea	Ueguchi-Tanaka et al. (2007)
slr1d-4	Nipponbare	DELLA protein dwarf mutant	*N*-methyl-*N*-nitrosourea	Asano et al. (2009)